

Effect of Temperature and Pressure on the Electron Paramagnetic Resonance Spectra of Substitutional Impurities in Cubic SrTiO₃

L. RIMAI, T. DEUTSCH, AND B. D. SILVERMAN

Research Division, Raytheon Company, Waltham, Massachusetts

(Received 6 August 1963; revised manuscript received 21 October 1963)

The electron paramagnetic resonance spectra of Fe³⁺, Gd³⁺, Eu²⁺, and Cr³⁺ in cubic SrTiO₃ have been studied as a function of hydrostatic pressure to 10 000 bars and as a function of temperature between 300 and 110°K. The optical spectrum Cr³⁺:SrTiO₃ has been examined at 4.2, 77, and 300°K. From a comparison of the pressure data for Fe³⁺ and Cr³⁺ with those for these ions in other hosts, we deduce that the local compressibility at the site occupied by these impurities is enhanced by a factor of two over the bulk compressibility. The isoelectronic ions Gd³⁺ and Eu²⁺ show a striking difference in the temperature dependence of the ground-state cubic field parameter, b_{40} . This difference is due to the polarization of the lattice by the uncompensated charge of Gd³⁺ and manifests itself as a Curie-Weiss term in the temperature dependence of b_{40} . This polarization effect is also seen in the temperature dependence of b_{40} for Fe³⁺. Theoretical justification for the temperature dependence of this term is given.

I. INTRODUCTION

AT room temperature, SrTiO₃ has the cubic perovskite structure¹ with 5 atoms per unit cell. In each unit cell there are two metal ions, Sr²⁺ and Ti⁴⁺. Small concentrations of certain ions of the two lower transition series may be incorporated into single crystals, and a number of papers dealing with the electron paramagnetic resonance (EPR) spectra of such impurities has been published in recent years.²⁻⁶ In most cases the valence of the impurity ion differs from that of either metal ion of the host. Nevertheless, a few of these transition ions do enter into the lattice as substitutional impurities. This is the case of the three *S*-state ions with which we are here concerned, namely, Fe³⁺, Gd³⁺, and Eu²⁺. Cr³⁺ also dissolves substitutionally. Mn⁴⁺, for which both valence and size match Ti⁴⁺, is not substitutional and therefore was not investigated.

Previous resonance studies disclosed some interesting facts about SrTiO₃. In the first place they revealed the presence of a phase transition in the host crystal, in the neighborhood of 110°K, which had not been detected in any other properties.^{2,4,5} This transition was later confirmed by birefringence studies and elastic constant measurements in undoped crystals.^{5,7} It was also found that the spin-Hamiltonian parameters for the isoelectronic di- and trivalent rare earths Eu²⁺ and Gd³⁺ differed considerably both in the cubic phase and in the low-temperature phase. For the *S*-state iron group ions Fe³⁺ and Mn²⁺, such a comparison was impossible, since Mn does not enter as an *S*-state ion

but as Mn⁴⁺.² However, the spin Hamiltonian for Fe³⁺ does not differ considerably from that in other cubic ionic crystals, in particular MgO.^{8,9}

The difference between the spin-Hamiltonian parameters for isoelectronic Eu²⁺ and Gd³⁺ led us to study these impurities more carefully, by varying the two parameters at our disposal, temperature, and pressure. The temperature data show that the extra charge on Gd³⁺ as well as on Fe³⁺ polarizes the lattice and manifests itself directly as a Curie-Weiss term in the temperature dependence of the spin-Hamiltonian parameter. The pressure data reveal no significant difference between the behavior of Eu²⁺ and Gd³⁺, suggesting that the perturbation mechanism involved is the same for each ion and allowing some cautious deductions concerning the dependence of the spin-Hamiltonian parameter on crystal field potential to be made.

The study of the optical spectrum Cr³⁺ ion, which is similar in size to Fe³⁺, was undertaken in order to detect any mechanism for binding the iron group ions into the host which is peculiar to SrTiO₃. The results indicated, however, that the effect of the ligands is not greater than in other ionic crystal hosts. The use of optical measurements to obtain the crystal field splitting of Cr³⁺ as a function of temperature and pressure, was precluded for practical reasons. The absorption bands were sufficiently broad and weak that we could detect no temperature shift and the pressure apparatus available was not suitable for optical measurements.

Both the pressure dependence of the Cr³⁺ *g* shift and Fe³⁺ cubic field parameter were measured. The former is much more simply related to the crystalline potential and serves as a check on the interpretation of the Fe³⁺ data.¹⁰⁻¹² The effect of pressure on these two ions is

¹ W. Känzig, in *Solid State Physics*, edited by F. Seitz and D. Turnbull (Academic Press Inc., New York, 1957), Vol. 4, p. 5.

² K. A. Müller, *Phys. Rev. Letters* **2**, 341 (1959).

³ K. A. Müller, 7ème Colloque Ampere, Arch. Sci. (Geneva) **11**, 150 (1958).

⁴ K. A. Müller, *Helv. Phys. Acta* **31**, 173 (1958).

⁵ L. Rimai and G. A. deMars, *Phys. Rev.* **127**, 702 (1962).

⁶ L. Rimai and G. A. deMars, in *Proceedings of the First International Conference on Electron Paramagnetic Resonance, Jerusalem, 1962* (Academic Press Inc., New York, 1963), Vol. I, p. 51.

⁷ R. O. Bell and G. Rupprecht, *Phys. Rev.* **129**, 90 (1963).

⁸ W. Low, *Proc. Phys. Soc. (London)* **B69**, 1169 (1956).

⁹ W. Low, in *Paramagnetic Resonance in Solids* (Academic Press Inc., New York, 1960).

¹⁰ W. M. Walsh, *Phys. Rev.* **122**, 762 (1961).

¹¹ W. M. Walsh, *Phys. Rev.* **107**, 905 (1957).

¹² W. M. Walsh, *Phys. Rev.* **114**, 1473 (1959).

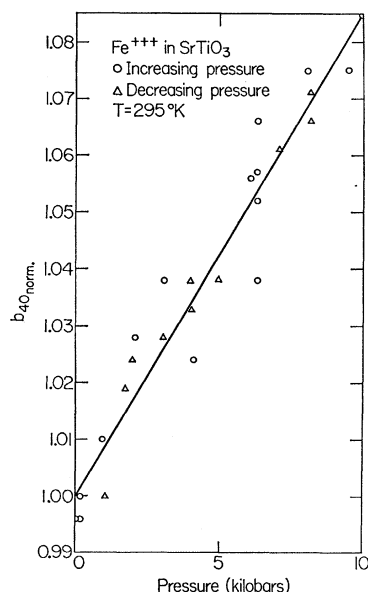


FIG. 1. Normalized b_{40} versus pressure for Fe^{3+} in SrTiO_3 .

much stronger in SrTiO_3 than in an MgO host.¹⁰ From a consideration of all the data on the iron group we are led to conclude that the compressibility at the Cr or Fe sites is about twice the bulk value.

In Sec. II we present a short account of the experimental techniques. The data are presented in Sec. III. In Sec. IV these data are discussed in view of the questions just mentioned. In the discussion of the polarization effect we use a phenomenological expression for which the theoretical justification is outlined in the Appendix.

II. COMMENTS ON THE EXPERIMENTAL TECHNIQUES

Microwave measurements were made at 16 and 35 kMc/sec; the latter frequency was used in the pressure measurements. At 35 kMc/sec a simple reflection spectrometer was employed and the microwave structure, consisting of a plug and shorted waveguide containing the sample, was generally used in a non-resonant fashion. Although matching was by no means perfect, measurements with good signal-to-noise ratio were possible using a 25-cps field modulated lock-in detection system. The klystron frequency was stabilized on an external cavity. The field was measured with a proton resonance gaussmeter. Attempts to employ the resonances of the microwave structure provided a better signal-to-noise ratio but were very inconvenient because the extreme pressure and temperature sensitivity of the sample dielectric constant caused appreciable shifts in the resonance frequency of the structure. The 16-kMc/sec spectrometer was a balanced bolometer type, of standard design. Its signal-to-noise ratio was good enough to permit observation of the absorption lines directly on a scope when the field was swept at a

low audio frequency. The temperatures of measurements between 300 and 110°K were obtained by establishing heat contact between the liquid-nitrogen chamber and the sample chamber of a He cryostat with a low pressure of He gas and introducing small amounts of liquid N_2 in the N_2 reservoir which was subsequently pumped out. By adjusting the He pressure and the amount of liquid N_2 , the desired temperatures could be reached and kept constant to within $\pm 2^\circ\text{K}$ for sufficient time to allow measurement of the line positions. The temperature was measured with a calibrated platinum thermometer.

The pressure apparatus was a modification of a system described in the literature¹³; pentane was used as the pressure transmitting fluid. The pressure was determined by measuring with a bridge the change in resistance of a manganin coil, which was calibrated using the freezing point of mercury at 0°C as 7640 kg/cm^2 . The pressure vessel used was made of W545 non-magnetic stainless steel (available from Westinghouse Electric Company, Materials Manufacturing Department, Blairsville, Pennsylvania); it was approximately $11\frac{1}{4}$ in. long, with an i.d. of $\frac{1}{2}$ in., an o.d. of $2\frac{1}{4}$ in. near the ends, and a 2 in. o.d. in the central portion. This design allowed the bomb to fit into the 2-in. gap between the tapered pole pieces of a 12-in. magnet while reinforcing the bomb at the ends where there are regions of high stress near the sealing holes.

Microwave radiation was introduced via a plug with a tapered sapphire window; this plug was essentially a scaled down version of a 24-kMc/sec unit described by Lawson and Smith.¹⁴ However, a conical sapphire impedance matching piece was used instead of the wedge described by Lawson. The sample was placed at the end of the piece of rectangular 35-kMc/sec waveguide $4\frac{1}{2}$ in. long and tuned by a copper shorting stub. The bomb and plug were tested to about 12 kbars and used regularly to 10 kbars.

The optical measurements on chromium-doped SrTiO_3 were made using a Perkin-Elmer grating

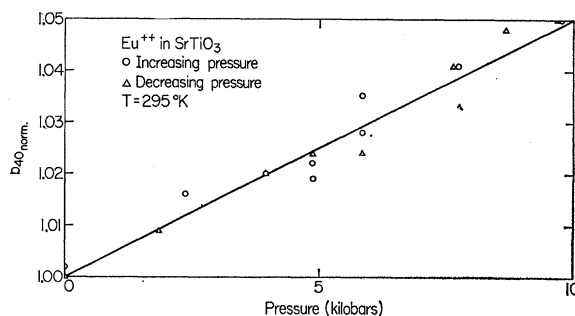


FIG. 2. Normalized b_{40} versus pressure for Eu^{2+} in SrTiO_3 .

¹³ D. Langer and D. M. Warschauer, Rev. Sci. Instr. 32, 32 (1961).

¹⁴ A. W. Lawson and G. E. Smith, Rev. Sci. Instr. 30, 989 (1959).

monochromator and a liquid-helium Dewar; measurements were made at 4.2, 77, and 300°K. The transmission of the sample was compared with that of undoped or "pure" material.

III. EXPERIMENTAL RESULTS

The spin Hamiltonian for *S*-state ions in crystal fields of cubic symmetry has the general form

$$\mathcal{H}(\mathbf{S}) = g\beta\mathbf{H}\cdot\mathbf{S} + b_{40}\left[Y_{40}(\mathbf{S}) + \frac{(70)^{1/2}}{14}(Y_{4,4} + Y_{4,-4})\right] + b_{60}\left[Y_{60}(\mathbf{S}) - \frac{(14)^{1/2}}{2}(Y_{6,4} + Y_{6,-4})\right] + \mathbf{A}\mathbf{I}\cdot\mathbf{S}, \quad (1)$$

where \mathbf{H} is the magnetic field, β the Bohr magneton, \mathbf{S} the spin of the ion, g the spectroscopic splitting factor, \mathbf{I} the nuclear spin, and the Y 's are spherical harmonics. b_{60} is zero for Fe³⁺ with 3*d* electrons and $S = \frac{5}{2}$; for both Gd³⁺ and Eu²⁺ $S = \frac{7}{2}$. The term $\mathbf{A}\mathbf{I}\cdot\mathbf{S}$

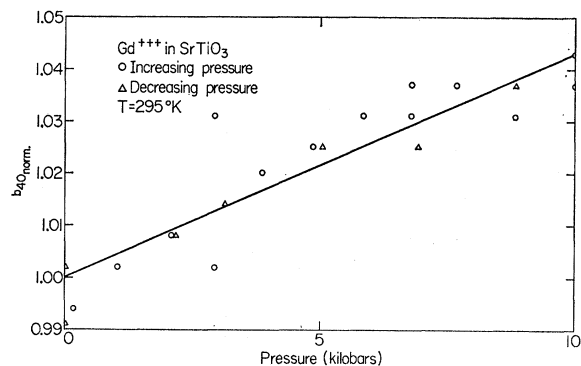


FIG. 3. Normalized b_{40} versus pressure for Gd³⁺ in SrTiO₃.

is appreciable only for the two Eu²⁺ isotopes, but even in this case the corresponding hyperfine structure was resolved only below 110°K.⁶ For $S = \frac{7}{2}$ $b_{60} \ll b_{40}$,^{5,6} and the increments in field separation due to increments in b_{60} were actually always negligible. From now on we shall therefore restrict the paper to results and discussion on the fourth-order cubic field parameter.

In Figs. 1–3 we show the room-temperature pressure dependence of b_{40} for the three ions, normalized to the value of b_{40} at one atmosphere. The straight lines represent the least-squares fit to the data.

In Fig. 4 we show the temperature dependence of b_{40} for Gd³⁺ in the cubic phase of the crystal. Each point is the statistical average of a number of measurements. Figure 5 shows a similar graph for iron. The solid lines are theoretical fits to the experimental points, obtained in a fashion discussed in the next section. The temperature dependence of b_{40} for Eu²⁺, $1/b_{40}(\partial b_{40}/\partial T)$ is $8.6 \times 10^{-6} \text{K}^{-1}$, a very small quantity when compared to the temperature dependence of Gd³⁺.

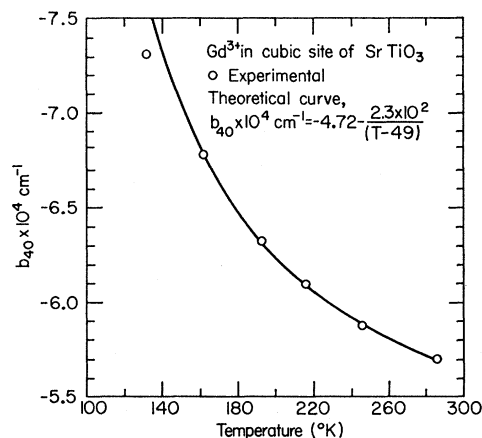


FIG. 4. Temperature dependence of b_{40} for Gd³⁺ in SrTiO₃; the experimental data are fitted with the phenomenological expression shown. The rms error at each point is comparable to the size of the circles.

In the discussion, the pressure dependences have been converted to volume dependences using the compressibility via the relation

$$\left(\frac{\partial \ln b}{\partial \ln V}\right)_T = \left(\frac{\partial \ln b}{\partial P}\right)_T \left(\frac{\partial P}{\partial \ln V}\right)_T = \left(\frac{\partial \ln b}{\partial P}\right)_T \times \frac{2c_{12} + c_{11}}{3}. \quad (2)$$

The values of the elastic constants are $c_{11} = 3.21 \times 10^{12}$ dyn/cm² and $c_{12} = 1.12 \times 10^{12}$ dyn/cm².¹⁵

The EPR spectrum of Cr in SrTiO₃ has been studied previously.³ We measured the pressure dependence of the g value in the hope of extracting from it the pressure dependence of the cubic crystal field parameter $10 Dq$; the assumptions that must be made to do this are considered in the discussion. Figure 6 shows the data. The accuracy of the measurements is relatively low

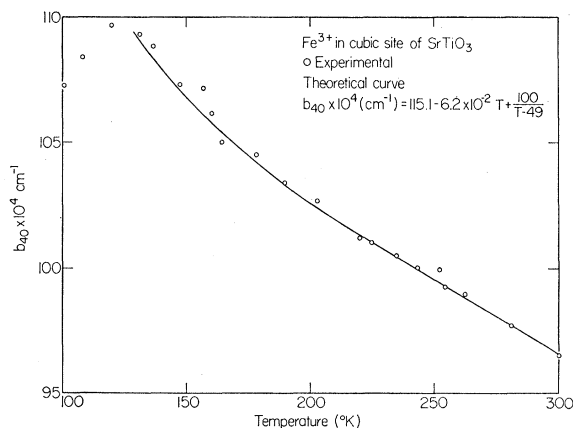


FIG. 5. Temperature dependence of b_{40} for Fe³⁺ in SrTiO₃. The points below 110°K are taken with the crystal in the tetragonal phase.

¹⁵ Data supplied by National Lead Company from whom the samples were purchased. See also Ref. 7.

TABLE I. The optical absorptions and some spectroscopic parameters for Cr³⁺ in three host crystals.

Transitions	Cr ³⁺ :SrTiO ₃		Cr ³⁺ :MgO		Cr ³⁺ :Al ₂ O ₃		Free Ion
	Measured	Predicted	Measured ^a	Predicted	Measured ^a	Predicted	
² E- ⁴ A ₂ (^β)	16 000 cm ⁻¹	15 500 cm ⁻¹	14 400 cm ⁻¹	14 000 cm ⁻¹	14 400 cm ⁻¹	15 300 cm ⁻¹	
² T ₁ - ⁴ A ₂ (^β)	16 800 cm ⁻¹	16 100 cm ⁻¹					
⁴ T ₂ (^{ρe})- ⁴ A ₂ (^β)	18 700 cm ⁻¹		16 200 cm ⁻¹		17 900 cm ⁻¹		
⁴ T ₁ (^{ρe})- ⁴ A ₂ (^β)	26 800 cm ⁻¹		22 700 cm ⁻¹		25 730 cm ⁻¹		
⁴ T ₁ (^{te})- ⁴ A ₂ (^β)		40 700 cm ⁻¹	29 700 cm ⁻¹	36 000 cm ⁻¹	39 100 cm ⁻¹	39 600 cm ⁻¹	
Parameter							
Dq		1879 cm ⁻¹		1620 cm ⁻¹		1790 cm ⁻¹	
B		750 cm ⁻¹		650 cm ⁻¹		630 cm ⁻¹	918 cm ⁻¹
$g_0 - g$	2.339 × 10 ⁻²		2.29 × 10 ⁻² ^b		$\frac{1}{3}(g_{11} + 2g_{12}) = 1.5 \times 10^{-2}$		
$10Dq(g_0 - g)$	55 cm ⁻¹		45 cm ⁻¹		40 cm ⁻¹		λ = 87 cm ⁻¹ ^c
8							

^a See Ref. 18. ^b See Ref. 10. ^c See Ref. 9.

for two reasons. Difficulties with the pressure measuring gauge caused a large error, estimated to be about $\pm 20\%$, in the pressure values. Second, the resonance line was not a pure absorption line, but a mixed one including some dispersion and the amount of mixing was pressure dependent. Hence there was some ambiguity in the location of the line center and consequently in the g value. The "mixed" resonance line is due to both spurious reflections from the pressure plug and variations in reflection coefficient due to the extreme pressure and temperature sensitivity of the dielectric constant of SrTiO₃. Nevertheless the data are sufficiently good to allow some useful deductions, primarily because the pressure shift is large, twice that for Cr³⁺ in MgO,¹⁰ and the linewidth is extremely small (~ 1 Oe).

A preliminary report on the optical spectrum of Cr³⁺ in SrTiO₃ was given by Müller.¹⁶ The results reported here were obtained independently and are essentially in agreement with Müller's results. We find that at 4.2°K there are two relatively intense bands about 800 cm⁻¹ wide centered at 18 700 and 26 800 cm⁻¹; there are also two absorptions, about 15 to 30 cm⁻¹ wide, centered at 16 000 and 16 800 cm⁻¹. As the temperature is increased the strong bands broaden and become somewhat weaker. The line at 16 000 cm⁻¹ does not change while the line at 16 800 cm⁻¹ seems to be somewhat stronger at the higher temperatures. At 4.2°K the 18 700 cm⁻¹ band shows structure which disappears at higher temperatures. The data are listed in Table I which appears in the discussion.

IV. DISCUSSION

A. Trivalent Chromium and Covalency Effects

There is no detailed theory relating the microwave splittings to the effects of the crystal field on the electronic states of the three S -state ions. It is also

difficult to study the optical spectra directly. There does exist, however, a considerable amount of theoretical and experimental work concerning trivalent chromium in a number of host crystals. Data for chromium in SrTiO₃ may be compared with that of several other host crystals to isolate any peculiarities arising from the SrTiO₃ host.

The optical data for Cr³⁺ in SrTiO₃ are tabulated in Table I along with experimental data for MgO and Al₂O₃ hosts; the transitions responsible for the absorptions are also tabulated. If the theory of Tanabe and Sugano^{17,18} is considered applicable, the fourth order cubic field parameter $10Dq$, the Racah parameter B , and the location of the two sharp lines corresponding to the ²T₁-⁴A₂ and ²E-⁴A₂ transitions may be calculated from the observed locations of the two intense absorption bands. The results of such a calculation for SrTiO₃ and for Cr³⁺:MgO and Cr³⁺:Al₂O₃ are also tabulated in Table I. The assignments for the two sharp lines in SrTiO₃ are doubtful for two reasons. First, the ²T₁-⁴A₂ transition has not been observed in other crystals; the increase in the strength of this transition with increasing temperature suggests it is normally

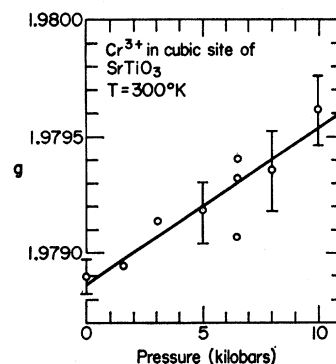


FIG. 6. Pressure dependence of g for Cr³⁺ in SrTiO₃. The data with errors correspond to statistical averages of a number of measurements at a given pressure. The other points correspond to isolated measurements.

¹⁶ K. A. Müller, in *Proceedings of the First International Conference on Electron Paramagnetic Resonance, Jerusalem, 1962* (Academic Press Inc., New York, 1963), Vol. I, p. 17.

¹⁷ Y. Tanabe and S. Sugano, *J. Phys. Soc. Japan* **9**, 753 (1954).

¹⁸ D. S. McClure, in *Solid State Physics*, edited by F. Seitz and D. Turnbull (Academic Press Inc., New York, 1959), Vol. 9.

forbidden and is allowed in SrTiO₃ because of phonon participation that does not usually occur. Second, the ²E—⁴A₂ line has been seen in emission in¹⁸ Cr³⁺:MgO and¹⁹ Cr³⁺:Al₂O₃, but we were unable to observe fluorescence in Cr³⁺:SrTiO₃. This may be due to the strong background absorption in SrTiO₃ which makes pumping ineffective, or to a short lifetime for the ²E level due to phonon assistance in an otherwise purely radiative decay.

The Tanabe and Sugano theory does not predict the optical absorptions from first principles, but rather assumes that the only effect of the host crystal is to alter the radial dependence of the 3*d* electron wave functions. The radial functions appear in the independent parameters of the theory. These parameters, *Dq* and *B*, may be obtained from any two of the bands observed. The inadequacy of theory is shown by the fact that different values of the parameters are obtained when different pairs of observed bands are used in the computation. This indicates that the angular portion of the wave function is changed due to the presence of the ligands.

Recently, detailed calculations have been performed using the molecular orbital approach for the cubic field splitting of particular transition ions in crystals.^{20,21} In particular, Lohr and Lipscomb²⁰ have calculated 10*Dq* for Cr³⁺ in various octahedral arrangements of O²⁻ neighbors. Their agreement with the experimental values in Al₂O₃, MgO, and beryl hosts is reasonable. Among the cases they considered is the one corresponding to an O²⁻ arrangement with no axial distortion, with the Cr-O distance of 1.94 Å, resulting in a value 10*Dq*=18 400 cm⁻¹. If we note that the Ti-O separation in SrTiO₃ and the Cr-O separation in LaCrO₃, which has the same structure as SrTiO₃, are both 1.95 Å, we expect that theory to apply to Cr substituted at a Ti site in SrTiO₃, and indeed it predicts the observed 10*Dq*, 18 700 cm⁻¹ quite well.

The shift of *g* from its spin only value yields information about the change in the electron wave functions from those in the free ion, and a comparison of this shift for chromium in various host crystals should indicate if there are any peculiarities in SrTiO₃. The free-ion ground term is a ⁴F which, in a cubic field, splits into an orbital singlet ⁴A₂ and two-orbital triplets ⁴T₂ and ⁴T₁. The singlet is the ground state in octahedrally coordinated sites. If it is assumed that the spin-orbit coupling energy may be written in terms of total spin and total angular momentum operators, **L** and **S**, as in the Russell-Saunders (R.S.) coupling scheme for free ions, the *g* shift of the ground state

may be written as^{21,19}:

$$\Delta g = g - g_0 = -\frac{2\lambda_{\text{cryst}}}{10Dq} \sum_{i=1}^3 \sum_{j=1}^3 \langle {}^4A_2 | L_i | j \rangle \langle j | L_i | {}^4A_2 \rangle, \quad (3)$$

where the perturbation theory takes into account only the effect of the first excited triplet. *j*=1, 2, or 3 are the three substates of the triplet and λ_{cryst} is a radial integral analogous to the free ion spin-orbit coupling constant λ of the R.S. coupling, except that crystal wave functions have to be used. The ligands affect this radial integral and also the angular momentum matrix elements. The radial integral, which involves 1/*r*³, where *r* is the 3*d* electron radius vector, will decrease due to the expansion of the *d* electron wave functions in the crystal. The matrix elements of *L_i* will in general also decrease due to the admixture of wave functions not centered at the nucleus of the magnetic ions.²¹ Deviation of 10*Dq*(*g*₀—*g*)/8 from the free-ion spin-orbit constant will be a measure of the degree of covalency and we have included its value in Table I. For Al₂O₃:Cr, the average $\frac{1}{3}(2g_{11} + g_{11})$ was used.

Since the wave functions enter the expressions for *B* and for the *g* shift in different ways, we do not expect the deviations of these quantities from their free-ion values to be in the same proportion and the table shows this. The variations in these two quantities from host to host are less than those in going from the free ion to any host. If there is any trend at all, the values in SrTiO₃ are somewhat closer to the free-ion ones. Hence one cannot invoke unusually strong covalent binding to explain the pressure effects on Cr³⁺ and Fe³⁺ in SrTiO₃.

Let us now consider the pressure dependence of the various parameters. For the case of hydrostatic pressure as applied to a cubic crystal where the ion positions in the unit cell are determined by symmetry considerations alone (substitutional impurities), the pressure effects on the spectroscopic parameters may be interpreted as effects due to a change in lattice constant. The bulk compressibility does not necessarily relate the change in pressure to the change in lattice constant in the vicinity of the impurity. This "local compressibility" is an extra variable that we have to contend with in the study of the data.

The spectroscopic parameters will depend on the lattice constant either through the various terms in the crystalline potential, or through the perturbation of the 3*d* (or 4*f*) wave functions by the presence of the ligands. Some parameters depend only on the latter (λ, *B*), others, like 10*Dq*, Δ*g*, *b*₄₀, on both. In the simplest model 10*Dq* is proportional to *V*₄₀, the cubic crystal field potential, and to ⟨*r*⁴⟩, where *r* is the 3*d* electron radius vector and the average is over the radial functions in the crystal. More realistically, as the calculations mentioned above show,^{20,21} 10*Dq* is a sum of contributions, of which only one, and not necessarily the largest one, is proportional to ⟨*r*⁴⟩*V*₄₀.

¹⁹ S. Sugano, A. L. Schawlow, and F. Varsanyi, Phys. Rev. **120**, 2045 (1960).

²⁰ L. L. Lohr and W. N. Lipscomb, J. Chem. Phys. **38**, 1607 (1963).

²¹ S. Sugano and R. G. Schulmann, Phys. Rev. **130**, 517 (1963).

TABLE II. A comparison of the volume dependences of Δg and Dq for chromium and nickel in MgO.

	$-\frac{V}{Dq} \frac{\partial Dq}{\partial V}$ ^a	$\frac{V}{\Delta g} \frac{\partial \Delta g}{\partial V}$ ^b
Cr ³⁺ :MgO	1.84	2.0
Ni ²⁺ :MgO	2.0	1.9

^a See Ref. 22.^b See Ref. 11.

The other terms represent admixtures of ligand orbitals not simply expressible as changes of the radial functions of the magnetic electrons. The presence of $\langle r^4 \rangle$ and of the latter contributions may entail deviations from the R^{-5} dependence (R is the lattice constant) for $10Dq$, predicted on the basis of only the V_{40} term.

In light of these two remarks let us examine Drickhamer's pressure data for the $10Dq$ of various transition ions in MgO and Al₂O₃.²²⁻²⁴ In Al₂O₃, when the bulk compressibility is used to obtain the dependence of Dq on lattice constant, it is found quite accurately to follow the R^{-5} law ($d \ln Dq / d \ln V = -5/3$). In MgO, on the other hand, there are deviations which vary from ion to ion. $-\frac{3}{5}(d \ln Dq / d \ln V)$ varies from about 1.1 for Co²⁺ and Cr³⁺ to as much as 1.6 for Ti³⁺. This could be ascribed to an enhanced local compressibility or to the covalency effects discussed above. Fortunately, for the one ion with which this work is mostly concerned, Cr³⁺, this effect is relatively small. Even in MgO the deviation of the logarithmic derivative from 5/3 is only 10% which is negligible when compared with the large effect to be dealt with for the SrTiO₃ host. The very small pressure dependence of the Racah parameter B for Cr³⁺ in^{23,24} MgO (a change of -20 parts in 650 in 150 kbars while Dq changes by $+20$ parts in 160) also indicates that the covalency effects are not too sensitive to small changes in lattice constant.

There is evidence from previous work showing that in general the change in Δg with pressure is mainly due to changes in $(Dq)^{-1}$ rather than the other factors in Eq. (3).¹⁰ Changes in the λ_{cryst} and in the matrix elements of L_z would be due to the volume dependence of covalency effects and are thus, by previous arguments, expected to be small. In addition, the volume dependence of Δg for Cr³⁺ and Ni²⁺ in MgO does indeed come out quite close to the volume dependence of Dq^{-1} for the same ions, as shown on Table II.^{10,22}

In this light we may consider the pressure dependence of Dq for Cr³⁺ in MgO as derived from the pressure dependence of Δg . This pressure dependence, combined

with the bulk compressibility, yields a volume dependence about twice as large as for the crystals studied previously. From the data discussed above, we have about the same covalency effects for Cr³⁺ in this crystal as in MgO and Al₂O₃. We therefore are left with only two possible explanations for this strong volume dependence: either the bulk compressibility used in computing the volume dependence from the measured pressure data does not describe the behavior near the magnetic ion and a larger, local compressibility must be used, or large polarization effects are operative. There are theoretical grounds to expect the latter to be present in SrTiO₃, since the impurity represents an extra charge which has no closeby compensation. These same grounds predict a strong temperature dependence for the polarization effects. Due to technical difficulties in performing a good temperature-dependent g -shift measurement in this crystal, the results on Fe³⁺, as discussed later, are invoked to show that such polarization effects should in general be too small to account for these results. It is, therefore, concluded that in SrTiO₃ the compressibility in the neighborhood of the Cr³⁺ is larger by about a factor of 2 from its value in MgO.

B. The Cubic Field Splitting of Fe³⁺

Next the results on b_{40} of Fe³⁺ are considered. As a basis for discussion, one again resorts to the comparison of data between SrTiO₃ and MgO, as displayed in Table III.

TABLE III. Comparison of the properties of iron and chromium in SrTiO₃ and MgO. The volume derivatives have been obtained from the pressure derivatives using the bulk compressibility.

	MgO	Cr ³⁺	SrTiO ₃
$\frac{1}{\Delta g} \frac{\partial \Delta g}{\partial P}$	$1.1 \times 10^{-6} \text{ (bars)}^{-1}$ ^a	$-2.6 \times 10^{-6} \text{ (bars)}^{-1}$ ^b	
$\frac{V}{g} \frac{\partial \Delta g}{\partial V}$ (Bulk comp.)	2.0 ^a	4.7 ^b	
$10Dq$	$16\,200 \text{ cm}^{-1}$ ^c	$18\,700 \text{ cm}^{-1}$ ^b	
	MgO	Fe ³⁺	SrTiO ₃
$\frac{1}{b_{40}} \frac{\partial b_{40}}{\partial P}$	$4.0 \times 10^{-6} \text{ (bars)}^{-1}$ ^a	$8.5 \times 10^{-6} \text{ (bars)}^{-1}$ ^b	
$\frac{V}{b_{40}} \frac{\partial b_{40}}{\partial V}$ (Bulk comp.)	-7.1 ^a	-15.4 ^b	
b_{40}	$+102.5 \times 10^{-4} \text{ cm}^{-1}$ ^c	$+96.14 \times 10^{-4} \text{ cm}^{-1}$ ^d	
$\frac{\partial \ln b_{40}}{\partial \ln V}$ ^e	3.6	3.3	
$\frac{\partial \ln Dq}{\partial \ln V}$			

²² H. G. Drickamer, in *Solids Under Pressure*, edited by Paul and Warschauer (McGraw-Hill Book Company, Inc., New York, 1963).²³ R. W. Parsons and H. G. Drickamer, *J. Chem. Phys.* **29**, 930 (1958).²⁴ S. Minomura and H. G. Drickamer, *J. Chem. Phys.* **35**, 903 (1961).^a See Ref. 10.^b Present work.^c See Ref. 9.^d See Ref. 4. The sign comes from later measurements privately communicated to the authors by Dr. K. A. Müller.^e See Eqs. (7) and (8).

TABLE IV. Measured values of the parameters b_{40} and b_{60} for Eu²⁺ and Gd³⁺ in several hosts and ionic contributions to the fourth- and sixth-order terms of the crystal potential in each host.

Host	Ion	b_{40}	b_{60}	$\frac{V_{40}}{\langle r^4 \rangle}$ in cm ⁻¹ (Å) ⁻⁴	$\frac{V_{60}}{\langle r^6 \rangle}$ in cm ⁻¹ (Å) ⁻⁶
CaF ₂	Eu ²⁺	57.9 × 10 ⁻⁴ cm ^{-1 a}	0.5 × 10 ^{-4 a}	-5.8 × 10 ²	0.50 × 10 ²
SrF ₂	Eu ²⁺	44.9 × 10 ^{-4 g}		-4.3 × 10 ²	0.42 × 10 ²
BaF ₂	Eu ²⁺	36.0 × 10 ^{-4 g}		-3.1 × 10 ²	0.26 × 10 ²
CaF ₂	Gd ³⁺	46 × 10 ⁻⁴ cm ^{-1 b}	-1.0 × 10 ^{-4 b}	-5.8 × 10 ²	0.50 × 10 ²
CdF ₂	Gd ³⁺	47.4 × 10 ⁻⁴ cm ^{-1 f}		-6.4 × 10 ²	0.55 × 10 ²
SrF ₂	Gd ³⁺	41.0 × 10 ⁻⁴ cm ^{-1 f}		-4.3 × 10 ²	0.42 × 10 ²
BaF ₂	Gd ³⁺	36.2 × 10 ⁻⁴ cm ^{-1 f}		-3.1 × 10 ²	0.26 × 10 ²
ThO ₂	Gd ³⁺	54.7 × 10 ^{-4 c}	0.26 × 10 ^{-4 c}	-9.7 × 10 ²	0.78 × 10 ²
SrTiO ₃	Eu ²⁺	106 × 10 ^{-4 d}	1.0 × 10 ^{-4 d}	-2.8 × 10 ²	
SrTiO ₃	Gd ³⁺	-5.7 × 10 ^{-4 e}	0.5 × 10 ^{-4 e}	(from 12 n. n. O ²⁻) and +3.7 × 10 ² (from 8 n. n. n. Ti ⁴⁺)	-0.58 × 10 ²

^a Ryter, Helv. Phys. Acta 30, 353 (1957).

^b W. Low, Phys. Rev. 109, 265 (1958).

^c W. Low and D. Shaltiel, Phys. Chem. Solids 6, 315 (1958).

^d See Ref. 6.

^e See Ref. 5.

^f See Ref. 32.

^g See Ref. 29.

In the parameterization of Tanabe and Sugano,¹⁷ b_{40} depends on many variables, B , C , Dq , λ , and the spin-spin interaction constants M_1 , M_2 .²⁵ Direct measurement of the optical spectrum of Fe³⁺ is hampered by the presence of strong charge transfer bands. This precludes the use of experimentally measured values for even the largest of these parameters. For this reason no detailed calculation of the b_{40} of Fe³⁺ exists. We have to use as a guide the calculations by Powell, Gabriel, and Johnston^{25,26} on isoelectronic Mn²⁺ from which it is concluded that if the parameters are varied in a reasonable range to cover practical cases, b_{40} is proportional to $\lambda^4 Dq^n$ with $3.4 < n < 6$ and is quite insensitive to changes in the other parameters. With the assumptions that the volume dependence of Dq does not vary appreciably between Cr³⁺, Ni²⁺ on one hand and Fe³⁺, Mn²⁺ on the other, and that the volume dependence of λ may be neglected, Walsh¹⁰ obtained $n = 3.6$ for both S -state ions. In passing we should note the following: Since a decrease in lattice spacing tends to spread the wave functions, therefore decreasing λ , $(\partial\lambda/\partial V) > 0$ and thus the $\partial \ln b_{40} / \partial \ln Dq$ so derived is rigorously only a lower bound for n . The dependence of λ on volume should, however, be similar to that of B , which for Cr³⁺ in MgO, implied $-(\partial \ln \lambda / \partial \ln V) \simeq \frac{1}{4}(\partial \ln Dq / \partial \ln V)$. Roughly speaking this means that due to the volume dependence of λ , n is at most 25% larger than $\partial \ln b_{40} / \partial \ln Dq$. Under similar assumptions we find, for Fe³⁺ in SrTiO₃ a value for this derivative which essentially agrees with that in MgO, as Table II shows. The values of b_{40} in the two different hosts are also essentially in agreement. Nevertheless, and again as for Δg in Cr³⁺, if the bulk compressibility of SrTiO₃ is used we find that the volume derivative of b_{40} , $\partial \ln b_{40} / \partial \ln V$ is twice as large as in MgO. This result

²⁵ M. J. D. Powell, J. R. Gabriel, and D. F. Johnston, Phys. Rev. Letters 5, 145 (1960).

²⁶ J. R. Gabriel, D. F. Johnston, and M. J. D. Powell, Proc. Roy. Soc. (London) A264, 503 (1961).

together with the corresponding one for Δg leads us to take the local compressibility for both Cr³⁺ and Fe³⁺ in SrTiO₃ about twice the corresponding local compressibility in MgO. This, it should be stressed, is coherent with all experimental results, independent of the detailed dependence of b_{40} on the optical parameters, and of the dependence of the optical parameters on covalency effects. Since it is inferred from the pressure dependence of Dq ²⁴ that the Cr³⁺ in MgO local compressibility differs from the bulk value by no more than 10%, it is concluded using values on Table III that for Cr³⁺ and Fe³⁺ substitutions in SrTiO₃, the ratio of local compressibility to bulk compressibility is 2.1 ± 0.15 .

This result implies that the spring constants connecting the Cr³⁺ or Fe³⁺ impurity to its neighbors have values appreciably smaller from those pertaining to Ti⁴⁺. This indicates that with sufficiently high doping these impurities may appreciably perturb the acoustic branch of the phonon spectrum in the range of frequencies

$$\omega \sim \omega_M \left[\frac{\text{bulk compressibility}}{\text{local compressibility}} \right]^{1/2} \simeq \frac{\omega_M}{\sqrt{2}},$$

where ω_M is the frequency of the mode with wave vector at the zone boundary.²⁷ This effect may also lead to phonon scattering by such impurities appreciably stronger than expected from the small atomic mass difference.

C. b_{40} for the Rare-Earth Ions

The theoretical problem of calculating the ground-state splittings of the S -state $4f^7$ shell is much more complicated, and at a much less developed stage than for the iron group S -state ions. The necessary spectroscopic data are scarcer, with practically none for divalent europium.¹⁸ The following discussion is,

²⁷ B. Mozer, Bull. Am. Phys. Soc. 8, 193 (1963).

TABLE V. The measured pressure dependences of b_{40} for Eu^{2+} and Gd^{3+} in SrTiO_3 and the volume dependences calculated from them.

	Gd	Eu
$\frac{1}{b_{40}} \frac{\partial b_{40}}{\partial P} \Big _{T=295^\circ\text{K}}$	$4.3 \times 10^{-6} \text{ (bars)}^{-1}$	$5.0 \times 10^{-6} \text{ (bars)}^{-1}$
$\frac{V}{b_{40}} \frac{\partial b_{40}}{\partial V} \Big _{T=295^\circ\text{K}}$	-7.8	-9.0

therefore, restricted to the qualitative level and makes use of the ionic point-charge model for the crystal field. This has a somewhat better foundation for the $4f$ shell than for the $3d$ shell, due to the better shielding of the magnetic electrons.

It will be assumed that the substitution takes place at the alkaline earth site. Ionic radii and bond length considerations lend support to this premise.²⁸ Table IV presents data on Gd^{3+} and Eu^{2+} in SrTiO_3 and some other cubic hosts where they substitute with preservation of local symmetry. The last two columns contain the calculated point charge potentials as they appear in the following expression:

$$V(\text{cubic}) = V_{40} \left[Y_{40} + \frac{(70)^{\frac{1}{2}}}{14} (Y_{4,4} + Y_{4,-4}) \right] + V_{60} \left[Y_{60} - \frac{(14)^{\frac{1}{2}}}{2} (Y_{6,4} + Y_{6,-4}) \right]. \quad (4)$$

The geometry was assumed to be that of the undistorted host. For the fluorite structure of CaF_2 and ThO_2 only the nearest neighbor anions need be considered. This situation does not prevail, however, for the perovskite crystal, as the table shows. Actually the nearest-neighbor approximation would give the wrong sign for V_{40} .

In the fluoride crystals there is certainly a good qualitative correlation between the values of b_{40} and V_{40} for both ions. For Eu^{2+} this correlation is very close to a linear law,²⁹ and it may be taken as proof that the perturbation mechanism which generates the fourth-order spin splitting represented by b_{40} is linear in the crystal potential V_{40} . The fact that for Gd^{3+} in these fluorides b_{40} is less sensitive to variations in V_{40} may be explained by distortions in the local crystal structure.²⁹ Since it has been shown that the smallest order of perturbation that produces a nonzero b_{40} is six³⁰⁻³² the fluoride data imply that if b_{40} depends linearly on V_{40} the other interaction constants occurring

in the expression for it are insensitive to variations of interatomic spacing.

The extrapolation of the linear relationship to the case of Eu^{2+} in SrTiO_3 does not work at all and seems to indicate that a radically different perturbation mechanism is operative. Although for Gd^{3+} the extrapolation to SrTiO_3 is qualitatively correct, this seems to be only a coincidence in view of the situation for Eu^{2+} . The dominance of a different mechanism in SrTiO_3 may be due to the anomalously small value of V_{40} , which is opposite in sign to that in the other hosts, and the relatively large value of V_{60} .

The pressure results as shown on Table V corroborate this idea of a different mechanism, since if one accepts a linearly dependence of b_{40} on V_{40} , the pressure data can only be explained by a local compressibility five times the bulk value. If it is still assumed that the only volume sensitive parameters on which b_{40} depends come from the ionic crystal field potential, if we disregard a possible contribution of V_{60} to b_{40} , and if bulk compressibility is used, we obtain for the exponent n in $b_{40} \propto V_{40}^n$ 4.7 for Gd^{3+} and 5.4 for Eu^{2+} .

D. Polarization Effects and Temperature Dependence of b_{40}

In the case of the trivalent ions we have to consider the perturbing effect on the lattice of the uncompensated charge which arises from the difference in valence. This uncompensated charge will cause a polarization in its neighborhood, i.e., the neighboring charges will be slightly displaced due to the electrostatic interaction between the uncompensated charge and the rest of the lattice. Such an effect is in principle present in any insulating host lattice. There is evidence, however, that it is small in crystals with normal (temperature independent) dielectric behavior. This evidence is partly in the previously cited pressure dependence of the optical spectra, and partly in the comparison between Mn^{2+} and Fe^{3+} in MgO . As is well known, SrTiO_3 has a very large dielectric constant which follows a Curie-Weiss law.¹ The large dielectric constant indicates that the material is strongly polarized by an applied electric field. One might then expect that temperature effects similar to those seen in the behavior of the dielectric constant of SrTiO_3 would appear in b_{40} due to the polarization of the lattice by the central field of a localized charge. The theory of this effect may be developed along lines similar to the dynamic theory of the dielectric constant for crystal lattices^{33,34} and is outlined in the Appendix: here we present the physical aspects of the phenomenon. For this purpose let us use the ionic model and neglect the electronic polariza-

²⁸ J. C. Slater, Quarterly Report in 46—Solid State and Molecular Theory Group, MIT, Report No. 1962 (unpublished).

²⁹ R. S. Title, Phys. Letters 6, 13 (1963).

³⁰ R. Lacroix, Helv. Phys. Acta 30, 374 (1957).

³¹ R. Lacroix, Proc. Phys. Soc. (London) 77, 550 (1961).

³² J. Sierrro, Phys. Letters 4, 178 (1963).

³³ W. Cochran, in *Advances in Physics*, edited by N. F. Mott (Taylor and Francis, Ltd., London, 1960), Vol. 9, p. 387; B. D. Silverman and R. I. Joseph, Phys. Rev. 129, 2062 (1963).

³⁴ It must be realized, however, that the spatial variation of the field of a point charge will couple to modes other than those of long wavelength.

bilities, which may be easily accounted for. The locally uncompensated charge causes small displacements of the neighboring ions. These may be calculated by adding to the lattice Hamiltonian the interaction energy of the ions with the extra charge. The ionic displacements will depend on the harmonic coupling constants. These displacements are assumed small and expanded in terms of linear combinations corresponding to the normal modes of the lattice. The energy including the new Coulomb term is rewritten in this way and minimized. Thus the displacements are found in terms of the frequencies and polarization vector of the normal modes. Each normal mode \mathbf{y} , j , contributes proportionally to $\omega_{\mathbf{y}j}^{-2}$ where $\omega_{\mathbf{y}j}$ is its frequency. The expressions for the displacements may be inserted in the formulas for the various spherical harmonic components of the crystal potential at the site of substitution. At a cubic site of a cubic crystal this symmetry will be preserved as long as there is no nearby localized charge compensation, and therefore the same terms will appear as in the undistorted situation. In general, for the coefficient V_{LM} of a given spherical harmonic $Y_{L,M}$ in the potential, we may write to lowest order in $(\omega_{\mathbf{y},j})^{-1}$

$$V_{LM} = V_{LM}^0 + \sum_{\mathbf{y},j} \frac{V_{LM}^{\mathbf{y},j}}{\omega_{\mathbf{y},j}^2}, \quad (5)$$

where $V_{LM}^{\mathbf{y},j}$ involves a sum over lattice sites and over the polarization vectors of the vibration \mathbf{y} , j . It also depends on various powers of R_i , the distance from each lattice site to the impurity site. Since V_{LM}^0 varies as $R_i^{-(L+1)}$ the $V_{LM}^{\mathbf{y},j}$ contains R_i^{-s} , with $s > (L+1)$ as expected for polarization effects. For normal crystals the $\omega_{\mathbf{y},j}$ have a small linear temperature dependence. For SrTiO₃, however, one mode j_0 has a strong temperature dependence. In particular for $\mathbf{y}=0$, $\omega_{0,j_0}^2 \propto (T - T_c)$ where T_c is the Curie temperature; this is the so-called soft mode corresponding to a transverse optical vibration. Neutron diffraction experiments show that this temperature dependence is approximately verified even for $\mathbf{y} \neq 0$.³⁵ Although the very long wavelength modes contribute negligibly to the ionic shifts of interest, other modes belonging to the same branch of the spectrum with $\mathbf{y} \approx 0$ and wavelength approaching that of the lattice parameter do contribute and introduce a term $(T - T_c)^{-1}$ in V_{LM} . The predominant temperature contribution to the crystal field from just these modes of the temperature-dependent branch is due to their relatively high density of states, large oscillator strengths and low frequencies.

We are therefore justified in writing the following phenomenological expression for the cubic potential at the impurity site,

$$V_{LM} = V_{LM}^0 + V_{LM}^1 T + \frac{V_{LM}^2}{T - T_c}. \quad (6)$$

Assuming that the second and third terms in (6) are

³⁵ R. A. Cowley, Phys. Rev. Letters **9**, 159 (1962).

small, we may also write, for an *S*-state ion:

$$v_{40} = b_0 + b_1 T + [b_2 / (T - T_c)]. \quad (7)$$

Equation (6) will correctly describe the temperature dependence of b_{40} even if other parameters such as λ are allowed to vary with lattice spacing. The reason is that the temperature dependence comes into the expressions for any parameter through the temperature dependence of the ionic displacements, in which these parameters are expanded.

In the case of Eu²⁺ the temperature dependence of b_{40} is absent to within experimental error. This is to be contrasted with the very strong dependence found for Gd³⁺ as seen in Fig. 4. The equality in volume dependences and the lack of temperature dependence for the divalent ion leads us to attempt to fit the Gd³⁺ data with a relation of the form (7) with $b_1 = 0$. The apparent success of this fit, as indicated by Fig. 4, does lend support to the idea of ascribing the enhanced temperature dependence of the trivalent ion to the polarization effect through the soft mode. We obtain³⁶

$$b_2 = -2.3 \times 10^{-2} \text{ cm}^{-1} (\text{°K}); \quad T_c = 49 \text{°K}. \quad (8)$$

Let us now consider the temperature dependence of b_{40} for Fe³⁺ in Fig. 5. We see that below about 190°K there is a small but measurable deviation from linearity. This deviation is rather small for an accurate curve fitting, such as was done for Gd³⁺. By assuming that this nonlinearity is entirely due to a polarization effect, we obtain the following values for the parameters in Eq. (7):

$$\begin{aligned} b_0 &= 115 \times 10^{-4} \text{ cm}^{-1}; \quad b_1 = -6.2 \times 10^{-6} \text{ cm}^{-1}/\text{°K}; \\ b_2 &= 100 \times 10^{-4} \text{ cm}^{-1}\text{°K}. \end{aligned} \quad (9)$$

Again we have assumed $T_c = 49 \text{°K}$.

Since the polarization vectors of the optical vibrations (in particular of the soft branch) are not known, it is impossible to calculate the temperature-dependent ionic displacements that could account for the portion of the b_{40} which follows the Curie-Weiss law. We can nevertheless make some comments on its sign and order of magnitude using point charge potentials. For either ion the absolute value of b_{40} is increased by the presence of this term. For the Ti⁴⁺ site the contributions to the fourth-order point charge potential, from both the nearest O²⁻ neighbors and the Sr²⁺ next nearest neighbors have the same sign. If one adopts the intuitive picture that the extra negative charge causes a repulsion of the O²⁻ and an attraction of the Sr²⁺, one concludes that an increase in the absolute value of the fourth-order potential and therefore of b_{40} can only come from the attraction of the Sr²⁺ ions. From the dependence of small changes of b_{40} on small changes of $10Dq$ and therefore of the fourth-order potential as discussed

³⁶ Report No. 6, U. S. Army Signal Corps, Fort Monmouth, New Jersey, Contract No. DA 36-039-sc-89126, 1963 (unpublished).

earlier, and from the fact that the next nearest neighbor contribution to $10 Dq$ is only a few percent, one may estimate that at 150°K the polarization effect of the extra charge displaces the Sr^{2+} about $10^{-2}a$ where a , the SrTiO_3 lattice constant, is 3.95 \AA .

For trivalent gadolinium we do not have an experimental measure of the dependence of b_{40} on the crystal field. The best that can be done is to estimate an equivalent change of lattice constant in the vicinity of the extra charge introduced by Gd^{3+} using the dependence of b_{40} on volume. This yields at 150°K a change of about $2 \times 10^{-2}a$. In this case, this crude calculation is most certainly not applicable, as the following argument will show: The sign and absolute value of V_{40} as shown on Table IV is a result of the contribution from the next nearest neighbor Ti^{4+} being larger and opposite in sign to that from the nearest neighbor O^{2-} . The extra $+1$ charge from the Gd^{3+} will, in the simple picture attract the O^{2-} and repel the Ti^{4+} , causing by either effect a decrease in the magnitude of V_{40} . However, the experimental results imply an increase in the magnitude of V_{40} from the polarization effect. To explain this one would have to invoke a strong $\text{O}^{2-}-\text{Ti}^{4+}$ coupling in such a way that both ions move towards the Gd^{3+} . One has to realize that the ionic displacements involved in the "soft mode" are probably much more complicated than independent ionic motions, and therefore predictions from such simple a model have to be taken with reservations even when they work. These complicating factors will not, however, affect the temperature dependence, as obtained by the calculations in the Appendix.

V. CONCLUDING REMARKS

This study of doped SrTiO_3 has revealed a number of interesting features which are summarized below.

(1) The pressure dependences of the Cr^{3+} g shift and of the Fe^{3+} b_{40} are found to be twice as large as in MgO . These results, coupled with the analysis of the Cr^{3+} optical data, led us to assign a local compressibility about twice the bulk value.

(2) The pressure dependence of the b_{40} for iso-electronic Gd^{3+} and Eu^{2+} has been measured, and similar values obtained for both ions. The pressure data cannot be reconciled with a linear dependence of b_{40} on V_{40} , such as seems to apply to the fluorides, indicating that a different mechanism operates in SrTiO_3 .

(3) The temperature dependence of the b_{40} for ions substituting with a locally uncompensated charge shows the presence of a polarization term due to interaction with the "ferroelectric" optical phonon branch. This effect was most strikingly exhibited by the difference between the temperature dependences of b_{40} for Gd^{3+} and Eu^{2+} . A formal theory for this effect, enabling one to calculate the corresponding ionic displacements and their temperature dependence is presented and used to fit the experimental data.

ACKNOWLEDGMENTS

We would like to thank G. A. deMars and Paul Guay for making the many spectrometer runs involved in obtaining the data. We are indebted to Miss Yvonne Blanchard for the optical measurements. Miss Winifred Doherty performed the least-squares fits to the pressure data. Finally, we would like to thank J. Silva and P. Oettinger for their efforts in helping build the pressure system.

APPENDIX A

In this section the calculation relating the change in crystal field potential (due to the presence of an uncompensated trivalent impurity) to the lattice frequencies will be outlined. Let Z be the charge of the impurity ion which is at a site originally occupied by a host ion of charge z . The origin of the coordinate system is chosen at the impurity site. The Hamiltonian of the system is the perfect crystal Hamiltonian plus the following perturbation term:

$$H^1 = \sum_{l,k} \frac{(Z-z)z_k}{|\mathbf{r}(\mathbf{k})|}, \quad (\text{A1})$$

$$\mathbf{r}(\mathbf{k}) = \mathbf{r}^0(\mathbf{k}) + \mathbf{u}(\mathbf{k}) = \mathbf{a}(l) + \mathbf{r}_k + \mathbf{u}(\mathbf{k}). \quad (\text{A2})$$

The notation that will be used is similar to that found in the book by Born and Huang.³⁷ $\mathbf{r}(\mathbf{k})$ is the instantaneous position of the k th type ion in the l th cell. This is composed of a vector $\mathbf{a}(l)$ to the unit cell, a vector \mathbf{r}_k to the k th ion of the basis, and a vector $\mathbf{u}(\mathbf{k})$ designating the displacement of the ion from its equilibrium position. Since the impurity ion substitutes at a center of symmetry in the crystal, its equilibrium position is the same as the position of the original host ion it replaces. The sum in Eq. (A1) is therefore over all the ions in the crystal except the impurity ion. The perturbation [Eq. (A1)] is then expanded in powers of the displacements $\mathbf{u}(\mathbf{k})$ with the use of Eq. (A2). The zeroth-order term, independent of the displacements $\mathbf{u}(\mathbf{k})$, represents the interaction of the excess impurity charge $(Z-z)$ with all other charges fixed at their initial equilibrium positions. This term has no effect upon the equations of motion for the ions and will be zero if there is charge compensation in some other region of the crystal.

The term linear in the displacements $\mathbf{u}(\mathbf{k})$ can be written

$$H_1^1 = \sum_{l,k,\alpha} \frac{\partial H^1}{\partial \mu_\alpha(\mathbf{k})} \mu_\alpha(\mathbf{k}) = \sum_{l,k,\alpha} \phi_\alpha(\mathbf{k}) \mu_\alpha(\mathbf{k}). \quad (\text{A3})$$

The nonvanishing of this term indicates that the ions are not stable at the equilibrium positions of the perfect lattice. The equilibrium positions are shifted due to the presence of the impurity charge. This is just the effect of interest.

³⁷ M. Born and K. Huang, *Dynamical Theory of Crystal Lattices* (Oxford University Press, New York, 1954).

The equation of motion for the system is

$$m_k \frac{d^2 \mu_\alpha(\mathbf{k})}{dt^2} = - \sum_{l' k' \beta} \phi_{\alpha\beta}(\mathbf{k}l') \mu_\beta(l') - \phi_\alpha(\mathbf{k}). \quad (\text{A4})$$

Performing the usual Fourier analysis of the motion and standard manipulations, one obtains the equation of motion for a mode of wave vector \mathbf{y} belonging to the j th branch.

$$\begin{aligned} \ddot{Q}(\mathbf{y}) + \omega^2(\mathbf{y}) Q(\mathbf{y}) + \frac{1}{N^{1/2}} \sum_{k, \alpha} \frac{1}{m_k^{1/2}} e_\alpha^*(k|\mathbf{y}) \left\{ \sum_l \exp[-2\pi i \mathbf{y} \cdot \mathbf{x}(l)] \phi_\alpha(\mathbf{k}) \right\}_{\text{reg}} \\ + \frac{1}{N^{1/2}} \sum_{k, \alpha} \frac{1}{m_k^{1/2}} I_\alpha^*(k|\mathbf{y}) \left\{ \sum_l \exp[-2\pi i \mathbf{y} \cdot \mathbf{x}(l)] \phi_\alpha(\mathbf{k}) \right\}_{\text{nonreg}} - \sum_{k, \alpha} \frac{z_k}{m_k^{1/2}} e_\alpha^*(k|\mathbf{y}) E_\alpha \exp(2\pi i \mathbf{y} \cdot \mathbf{x}_k) = 0. \quad (\text{A5}) \end{aligned}$$

The last term in this equation arises from the nonregular part of the Coulomb interaction between the ions that is incorporated into the equations of motion by introducing the macroscopic field. The regular part of this interaction gives rise to the so-called "inner field" which is incorporated into the frequencies $\omega^2(\mathbf{y})$. Similarly, the impurity-lattice interaction consists of a regular and nonregular part. This separation has been performed by the subscript labeling of the curly brackets in Eq. (A5). The regular part of the point-charge interaction can be used to explicitly define new equilibrium positions for the ions. Next, the following transformation is performed:

$$Q(\mathbf{y}) = q(\mathbf{y}) + d(\mathbf{y}). \quad (\text{A6})$$

The $q(\mathbf{y})$ are chosen as the displacements about the new equilibrium positions. Since the macroscopic field is a function of the ionic displacements, there will be a contribution from the last term in Eq. (A5) which arises from the ionic shifts described by the $d(\mathbf{y})$. This contribution will combine with the nonregular part of the impurity-lattice interaction [fourth term in Eq. (A5)] to yield the macroscopic field of a point charge in a dielectric medium which will be denoted by E_α^0 .

The shift of the coordinate of the mode of wave vector \mathbf{y} belonging to the j th branch is

$$d(\mathbf{y}) = - \frac{1}{N^{1/2}} \frac{1}{\omega^2(\mathbf{y})} \sum_{k, \alpha} \frac{1}{m_k^{1/2}} e_\alpha^*(k|\mathbf{y}) \left\{ \sum_l \exp[-2\pi i \mathbf{y} \cdot \mathbf{x}(l)] \phi_\alpha(\mathbf{k}) \right\}_{\text{reg}} + \frac{1}{\omega^2(\mathbf{y})} \sum_{k, l} \frac{z_k}{m_k^{1/2}} e_\alpha^*(k|\mathbf{y}) E_\alpha^0 \exp(2\pi i \mathbf{y} \cdot \mathbf{x}_k), \quad (\text{A7})$$

which leads to the following α th component of displacement of the k th type ion in the l th cell:

$$\begin{aligned} d_\alpha(\mathbf{k}) = - \frac{1}{N m_k^{1/2}} \sum_{\mathbf{y}} \sum_i \sum_{k', \beta} \frac{1}{\omega^2(\mathbf{y})} \frac{1}{m_{k'}^{1/2}} \left\{ \sum_{l'} \phi_\beta(k'l') \exp[-2\pi i \mathbf{y} \cdot \mathbf{x}(l')] \right\}_{\text{reg}} \exp[2\pi i \mathbf{y} \cdot \mathbf{x}(\mathbf{k})] \epsilon_\beta^*(k'|\mathbf{y}) \epsilon_\alpha(k|\mathbf{y}) \\ + \frac{1}{(N m_k)^{1/2}} \sum_{\mathbf{y}} \sum_i \sum_{k', \beta} \frac{1}{\omega^2(\mathbf{y})} \frac{z_{k'}}{m_{k'}^{1/2}} E_\beta^0 \exp[2\pi i \mathbf{y} \cdot \mathbf{x}(\mathbf{k})] \epsilon_\beta^*(k'|\mathbf{y}) \epsilon_\alpha(k|\mathbf{y}). \quad (\text{A8}) \end{aligned}$$

Note: $\epsilon_\alpha(k|\mathbf{y}) = e_\alpha(k|\mathbf{y}) \exp(2\pi i \mathbf{y} \cdot \mathbf{x}_k)$. The displacements of the ions due to the presence of an uncompensated net charge are written as the sum of two terms. The second term arises from the treatment of the continuum problem, i.e., a point charge in a dielectric medium. This is the predominant term at distances far from the impurity, i.e., distances very large compared with the lattice parameter. The first term gives the deviations from the dielectric formulation of the problem. This term is predominant at small distances, i.e., distances comparable with the lattice parameter. Since the relevant crystalline field term discussed in this paper transforms as $Y_{40} + (\sqrt{70}/14)(Y_{4,4} + Y_{4,-4})$, only ions in the vicinity of the impurity contribute significantly to this crystalline field term, and hence the major contributions to the pertinent displacements arise from the first term in Eq. (A8).

The paramagnetic electrons are subject to the following crystalline field potential at the position \mathbf{r} (in the point-charge approximation):

$$V = \sum_{l, k} \frac{z_k}{|\mathbf{r}(\mathbf{k}) - \mathbf{r}|}. \quad (\text{A9})$$

The position of the k th type ion in the l th cell can be written as the position of this ion in the perfect crystal $\mathbf{r}^0(\mathbf{k})$ plus the shift $\mathbf{d}(\mathbf{k})$. The first term in such expansion, independent of $\mathbf{d}(\mathbf{k})$, is just the usual crystalline potential term arising from the undistorted lattice. The next term in the expansion, the term linear in the $\mathbf{d}(\mathbf{k})$, can be

written

$$\begin{aligned}
 V_1 = & -4\pi \sum_{l,k} \sum_{l_1 l_2 l_3} \sum_{l' l'' l'''} z_k \frac{\mathbf{d}(\mathbf{k}) \cdot \mathbf{r}^0(\mathbf{k})}{|\mathbf{r}^0(\mathbf{k})|^3} (-1)^{l''} (2l+1) \begin{pmatrix} l_1 & l_2 & l' \\ 0 & 0 & 0 \end{pmatrix}^2 \begin{pmatrix} l' & l_3 & l'' \\ 0 & 0 & 0 \end{pmatrix}^2 Y_{l' m'}^*(\theta_3 \psi_3) s^{l_1+l_2+l_3} Y_{l' m}(\theta_2 \psi_2) \\
 & + \frac{8\pi^{3/2}}{3^{1/2}} \sum_{l,k} \sum_{l_1 l_2 l_3} \sum_{l' l'' l''', m m'' m'''} z_k \frac{|\mathbf{d}(\mathbf{k})| |\mathbf{r}|}{|\mathbf{r}^0(\mathbf{k})|^3} Y_{1m}^*(\theta_1 \psi_1) Y_{l' m'}^*(\theta_3 \psi_3) (-1)^{l''} (2l+1) [(2l''+1)(2l'''+1)]^{1/2} s^{l_1+l_2+l_3} \\
 & \times \begin{pmatrix} l_1 & l_2 & l' \\ 0 & 0 & 0 \end{pmatrix}^2 \begin{pmatrix} l' & l_3 & l'' \\ 0 & 0 & 0 \end{pmatrix}^2 \begin{pmatrix} 1 & l'' & l''' \\ 0 & 0 & 0 \end{pmatrix} \begin{pmatrix} 1 & l'' & l''' \\ m & m'' & m''' \end{pmatrix} Y_{l''' m'''}^*(\theta_2 \psi_2). \quad (\text{A10})
 \end{aligned}$$

The crystalline potential has been expanded in spherical harmonics. θ_1 , θ_2 , and θ_3 are the angles between $\mathbf{d}(\mathbf{k})$, \mathbf{r} , $\mathbf{r}^0(\mathbf{k})$, and the z direction, respectively. The bracketed terms are $3j$ symbols.

If Eq. (A8) (the ionic shifts) is substituted into Eq. (A10) (crystal field potential), one obtains the frequency dependence as exhibited in the second term on the right side of Eq. (5) and an explicit expression for the $V_{LM}^{y,i}$.

Negative Resistance and Impact Ionization Impurities in n -Type Indium Antimonide*

R. J. PHELAN, JR.,[†] AND W. F. LOVE
University of Colorado, Boulder, Colorado
 (Received 2 May 1963)

n -type indium antimonide crystals at liquid-helium temperatures placed in magnetic fields of a few kilogauss have yielded negative resistance characteristics. The negative resistance is attributed to impact ionization of impurities. In addition, delay and rise times for the current have been studied, and an explanation in terms of the rate equation for ionization and recombination is given.

I. INTRODUCTION

THE initial impetus for studying this negative resistance characteristic came from the observation of oscillations of current and voltage generated by single crystals of n -type indium antimonide. These oscillations were previously observed by Haslett and Love¹ while studying the magnetoresistance of n -InSb in pulsed magnetic fields at liquid-helium temperatures. Studies of Sladek² and others have indicated that freezeout of the carriers occurs in InSb with the application of a magnetic field at liquid-helium temperatures and with subsequent application of sufficient electric fields impact ionization of the impurities may be obtained. McWhorter and Rediker³ have demonstrated that impact ionization of impurities in germanium can lead to a negative resistance characteristic. Here we add the observation of negative resistances in n -InSb involving freezeout and impact ionization.

II. SAMPLES

The n -InSb that was used for this study was from three single crystals. The original sample which demonstrated the negative resistance contained few excess donors. A second sample contained $4.6 \times 10^{14} \text{ cm}^{-3}$ excess donors and a Hall mobility of $9.1 \times 10^5 \text{ cm}^2 \text{ V}^{-1} \text{ sec}^{-1}$ at 77°K . The third source was from Cominco and contained relatively few excess donors, $9.5 \times 10^{13} \text{ cm}^{-3}$, and a Hall mobility of $2.7 \times 10^5 \text{ cm}^2 \text{ V}^{-1} \text{ sec}^{-1}$ at 77°K .

The original sample, shaped into a rectangular bar using a diamond saw, had potential and current leads soldered with indium solder. For the rest of the studies tellurium-doped gold wires were bonded to crystals cut with air-abrasive techniques and the contacts reliably showed linear current-voltage characteristics at liquid-nitrogen temperatures. Contacts were placed at various positions along the bars to check for inhomogeneities. All samples were etched in an attempt to eliminate surface effects.

III. EXPERIMENTAL RESULTS

A. Current-Voltage Characteristics

A typical set of current-voltage curves is given in Fig. 1. This is a Polaroid photograph of two traces of a Tektronix dual beam oscilloscope. Voltages are plotted

* Work supported by the U. S. Army.

[†] Present address: MIT Lincoln Laboratory.

¹ J. C. Haslett and W. F. Love, *Phys. Chem. Solids* **8**, 518 (1959).

² R. J. Sladek, *Phys. Chem. Solids* **5**, 157 (1958).

³ A. L. McWhorter and R. H. Rediker, *Proceedings of the International Conference on Semiconductor Physics, 1960* (Czechoslovakian Academy of Sciences, Prague, 1961, Academic Press Inc., New York, 1961), p. 134.